

Published in final edited form as:

Dev Cell. 2011 August 16; 21(2): 301–314. doi:10.1016/j.devcel.2011.06.033.

Semaphorin-PlexinD1 Signaling Limits Angiogenic Potential via the VEGF Decoy Receptor sFlt1

Tomasz Zygmunt^{1,*}, Carl Michael Gay^{1,*}, Jordan Blondelle², Manvendra K. Singh³, Kathleen McCrone Flaherty¹, Paula Casey Means¹, Lukas Herwig⁴, Alice Krudewig⁴, Heinz-Georg Belting⁴, Markus Affolter⁴, Jonathan A. Epstein^{3,5}, and Jesús Torres-Vázquez¹

¹Helen L. and Martin S. Kimmel Center for Biology and Medicine at the Skirball Institute, Dept. of Cell Biology, New York University School of Medicine, New York, 10016, USA ²Université Diderot-Paris 7, Paris, France ³Dept. of Cell and Developmental Biology, Cardiovascular Institute, University of Pennsylvania, Philadelphia, Pennsylvania 19104, USA ⁴Biozentrum, University of Basel, CH-4056 Basel, Switzerland ⁵Institute for Regenerative Medicine, University of Pennsylvania, Philadelphia, Pennsylvania 19104

Summary

Sprouting angiogenesis expands the embryonic vasculature enabling survival and homeostasis. Yet how the angiogenic capacity to form sprouts is allocated among endothelial cells (ECs) to guarantee the reproducible anatomy of stereotypical vascular beds remains unclear. Here we show that *Sema-PlxnD1* signaling, previously implicated in sprout guidance, represses angiogenic potential to ensure the proper abundance and stereotypical distribution of the trunk's Segmental Arteries (SeAs). We find that *Sema-PlxnD1* signaling exerts this effect by antagonizing the pro-angiogenic activity of Vascular Endothelial Growth Factor (VEGF). Specifically, *Sema-PlxnD1* signaling ensures the proper endothelial abundance of *soluble flt1* (*sflt1*), an alternatively spliced form of the VEGF receptor Flt1 encoding a potent secreted decoy. Hence *Sema-PlxnD1* signaling regulates distinct but related aspects of angiogenesis: the spatial allocation of angiogenic capacity within a primary vessel and sprout guidance.

INTRODUCTION

Blood vessels form a pervasive tubular network that distributes oxygen, nutrients, hormones and immunity factors. The first blood vessels assemble *de novo* via EC coalescence or vasculogenesis. Later, they expand via angiogenesis, the growth of new blood vessels from preexisting ones. In some locales this process is stereotypic and vascular sprouts form with evolutionarily conserved and organ-specific distribution, abundance and shapes (Carmeliet,

© 2011 Elsevier Inc. All rights reserved.

Address correspondence and material requests to J.T-V (Jesus.Torres-Vazquez@med.nyu.edu).

*Equal contribution.

The authors declare no competing financial interests.

Author Contributions

T.Z., C.M.G., J.T-V. (ideas, experiments, data analysis, fish lines, plasmids, writing); J.B., C.M. (experiments, data analysis); K.M.F. (experiments, fish lines, husbandry support, writing); M.S. (ideas, cell culture experiments, data analysis, writing); L.H., A.K., H-G. B., M.A. (*Tg(fliex:gal4ff)^{Ubs4}* line); J.A.E. (ideas, data analysis). All authors commented on the manuscript.

Publisher's Disclaimer: This is a PDF file of an unedited manuscript that has been accepted for publication. As a service to our customers we are providing this early version of the manuscript. The manuscript will undergo copyediting, typesetting, and review of the resulting proof before it is published in its final citable form. Please note that during the production process errors may be discovered which could affect the content, and all legal disclaimers that apply to the journal pertain.

2005; Isogai et al., 2001; Isogai et al., 2003). For example, zebrafish SeAs sprout bilaterally from the trunk's aorta just anterior to each somite boundary (SB; Figure 1A). SeA sprouts contain migratory, proliferative and filopodia-rich arterial angiogenic ECs molecularly distinct from the sedentary "phalanx" ECs remaining in the aorta (De Bock et al., 2009; Siekmann and Lawson, 2007; Torres-Vazquez et al., 2004). Normally, only aortic ECs near SBs acquire angiogenic capacity (Ahn et al., 2000; Childs et al., 2002). It is thought that non-endothelial paracrine VEGF signals promote angiogenic capacity, while Notch-mediated lateral inhibition between ECs antagonizes it (Phng and Gerhardt, 2009; Siekmann et al., 2008). However, the mRNA expression of *vegf-a* and Notch pathway genes is inconsistent with the distribution of SeA sprouts. *vegf-a* is not transcribed along SBs, but rather expressed dorsal to the aorta at both the flanking somites' centers and the hypochord, a midline endodermal cell row. Notch pathway genes are expressed continuously along the aorta or broadly through the body (Hogan et al., 2009b; Lawson et al., 2002; Leslie et al., 2007; Phng et al., 2009; Siekmann and Lawson, 2007) (C.M.G., J.B. and J. T-V., unpublished observations). Hence, other cascades likely modulate VEGF and/or Notch signaling at pre-sprouting stages to enable the stereotypical allocation of angiogenic capacity within the aorta. Perturbing these unidentified cascades might change the SeA sprouts' reproducible number, distribution and/or the ratio of aortic ECs that acquire angiogenic capacity.

Besides VEGF and Notch activity, proper SeA development requires paracrine Sema-Plxn signaling. Type 3 semas (*sema3s*) are repulsive guidance cues secreted by somites. *Sema3s* direct SeA sprout pathfinding by modulating cytoskeletal dynamics via the endothelial *Sema3*-receptor *PlxnD1*. Hence, *sema3* or *plxnD1* inactivation yields similar SeA sprout pathfinding defects in zebrafish and mice (Gay et al., 2011). Two observations made in zebrafish make Sema-*PlxnD1* signaling a candidate modulator of angiogenic capacity. First, *sema3* and *plxnD1* expression begins hours before SeAs sprout from the aorta at ~21 hours post-fertilization (hpf). Second, loss of Sema-*PlxnD1* signaling induces ectopic SeA sprout launching (Childs et al., 2002; Torres-Vazquez et al., 2004).

In wild type (WT) animals SeA sprouts grow dorsally with a chevron-like shape, bifurcate anteroposteriorly at the neural tube's roof level and interconnect with their ipsilateral neighbors at ~32 hpf forming the paired Dorsal Longitudinal Anastomotic Vessels (DLAVs) (Isogai et al., 2003). In contrast, in *plxnD1* (*out of bounds - obd*) mutants and *plxnD1* morphants, SeA sprouts are misshaped and interconnect ectopically with their ipsilateral neighbors but form properly placed DLAVs (Childs et al., 2002; Torres-Vazquez et al., 2004). Thus, we further examined Sema-*PlxnD1*'s signaling role during zebrafish SeA development, finding that it plays a pre-sprouting role as a repressor of the aorta's angiogenic potential - the probability that ECs acquire angiogenic capacity. This role stems from its ability to promote *sflt1*'s endothelial abundance and thus antagonize pro-angiogenic VEGF activity (Rahimi, 2006). We propose that Sema-*PlxnD1* signaling allocates angiogenic capacity among aortic ECs in a reproducible spatial pattern, guaranteeing the proper abundance and distribution of SeA sprouts.

RESULTS

Lack of Sema-*PlxnD1* signaling induces too many and ectopic SeA sprouts

To investigate if Sema-*PlxnD1* signaling modulates angiogenic capacity we measured SeA sprout abundance and positioning in WT and *obd* at 23 hpf, when individual *obd* SeA sprouts are readily identifiable as they are yet to interconnect ectopically. We found *obd* has almost twice the WT's number of SeA sprouts, with most of them launching ectopically (Figure 1A–D). Hence, Sema-*PlxnD1* signaling limits the abundance and defines the position of SeA sprouts.

To molecularly verify the angiogenic character of ECs within *obd* SeA sprouts we used whole mount RNA *in situ* hybridization (WISH) (Moens, 2008) to visualize expression of the pan-endothelial marker *cdh5* (Larson et al., 2004) and *flt4/vegfr-3*, which labels arterial angiogenic ECs within SeA sprouts and the vein (Covassin et al., 2006; Hogan et al., 2009b; Siekmann and Lawson, 2007). *flt4* is expressed in all SeA sprouts and vein of WT and *obd* (Figure 1E–F), confirming the angiogenic character of ECs within *obd*'s SeA sprouts and the lack of artery/vein differentiation defects in *obd* (Torres-Vazquez et al., 2004).

Loss of Sema-PlxnD1 signaling yields more angiogenic cells

To determine if *obd*'s SeA sprout overabundance is associated with too many angiogenic ECs we compared the number of EC nuclei found within developing SeAs and DLAVs of WT and *obd* at 21, 23 and 32 hpf. We found that *obd*'s SeAs/DLAVs collectively harbor more angiogenic ECs than WT (Figure S1A–B). We next aimed to compare the WT and *obd* ratios of angiogenic to phalanx arterial ECs. However, SeA sprouts arise while the aorta and vein segregate from each other (Herbert et al., 2009), making the quantification of early aortic EC abundance unfeasible. We thus instead counted EC nuclei in the axial vasculature (aorta and vein taken together) and found that *obd* shows increased axial vasculature EC abundance (Figure S1A–B). Hence, loss of Sema-PlxnD1 signaling yields more angiogenic and axial vasculature ECs.

Sema-PlxnD1 signaling is cell-autonomously required within the endothelium

To ask if Sema-PlxnD1 signaling acts cell autonomously to limit the number and define the position of SeA sprouts we performed cell transplants (Carmany-Rampey and Moens, 2006) to make heterogenotypic WT:*obd* (WT-to-*obd* and *obd*-to-WT) chimeras. We analyzed these at ~32 hpf to determine SeA sprout abundance and distribution and examine the SeA contribution of ECs from donors and hosts (Figure 1G–H). We found too many SeA sprouts in WT:*obd* chimeras. As in *obd*, some SeA sprouts launched ectopically and others were positioned correctly. WT ECs were found only within properly positioned SeA sprouts, while *obd* ECs contributed to misshapen SeAs sprouts at both ectopic and correct positions (Figure 1G–H and S1C). Control homogenotypic (WT-to-WT and *obd*-to-*obd*) chimeras also showed mosaic SeAs with both host and donor ECs (Figure S1E). Hence, SeAs are not necessarily of clonal origin, in agreement with results from prior transplantation and mosaic transgenic labeling experiments (Childs et al., 2002; Siekmann and Lawson, 2007).

obd ECs found within WT hosts contribute to SeAs/DLAVs much more often than WT ECs contribute to these angiogenic vessels in *obd* hosts (Figures S1C–D and S2C). Since *obd* ECs show exacerbated angiogenic capacity in a WT environment this property is not caused by axial vasculature EC over-abundance. Finally, non-endothelial *obd* cells, like ventral somitic muscle fibers (Childs et al., 2002), did not influence the abundance, distribution or anatomical patterning of SeA sprouts (Figure S1C), consistent with *plxnD1*'s endothelial-specific expression (Torres-Vazquez et al., 2004) and the identical vascular phenotypes of mice with global or EC-specific *plxnD1* inactivation (Gay et al., 2011). Thus, Sema-PlxnD1 signaling acts cell autonomously within the endothelium to limit angiogenic potential and ensure the proper abundance and positioning of SeA sprouts.

Aortic ECs with less Sema-PlxnD1 signaling (*obd*+/+) become angiogenic tip cells more often and are enriched in the aorta's dorsal side

Each SeA sprout has a spearheading tip cell that becomes “T” shaped during DLAV formation and which is trailed by a few stalk cells (Siekmann and Lawson, 2007). Tip cells embody an enhanced angiogenic state promoted by increased pro-angiogenic signaling and characterized by exacerbated filopodia dynamics whose acquisition and/or maintenance

involves cell competition (Jakobsson et al., 2010; Leslie et al., 2007; Roca and Adams, 2007).

Thus, if *Sema-PlxnD1* signaling antagonizes angiogenic potential then ECs with reduced *Sema-PlxnD1* signaling levels should acquire an enhanced angiogenic state more often. To test this hypothesis we used cell transplantation experiments to compare the properties of ECs from WT and *obd/+* heterozygotes. These embryos have the same number of ECs within both the SeAs/DLAVs and the axial vasculature (Figure S2A) and identical SeA sprout abundance, positioning and patterning (Figure 2A–B). We determined the frequency at which donor ECs become tip cells in homogenotypic (WT-to-WT and *obd/+*-to-*obd/+*) and heterogenotypic (WT-to-*obd/+* and *obd/+*-to-WT) chimeras. To ensure competition between donor and host ECs had occurred we only scored mosaic SeAs harboring both donor and host ECs. All chimeras showed correctly patterned and positioned SeA sprouts (Figure 2C–D and data not shown) and both kinds of homogenotypic chimeras showed identical donor tip cell percentages (Figure 2E). In contrast, the donor tip cell percentage was significantly larger in *obd/+*-to-WT chimeras and smaller in WT-to-*obd/+* chimeras (Figure 2E).

Hence, the angiogenic capacity and angiogenic positional fate of aortic ECs is not pre-specified but is acquired and/or maintained competitively, agreeing with prior related observations (Jakobsson et al., 2010; Siekmann and Lawson, 2007). Indeed, within developing SeA sprouts angiogenic cell nuclei swap positions (Movie S1), suggesting that angiogenic cells within SeA sprouts can exchange places. Thus, the SeA tip cell population scored in Figure 2C–E likely includes both the angiogenic cells that launched first from the aorta and kept their leading position and those that trailed the original tip cell but later overtook it. Prior studies suggest that migration speed is similar between cells with differential abilities to acquire/maintain a tip cell positional status (Jakobsson et al., 2010). Of note, both WT and *obd/+* embryos form DLAVs at similar times, suggesting that their SeA sprouts grow with matching speeds. Thus, independently of its roles in guiding SeA sprouts (Gay et al., 2011) and limiting EC abundance (Figure S1A–B), *Sema-PlxnD1* signaling antagonizes angiogenic responses.

Both the angiogenic potential of *obd* ECs and the angiogenic response of *obd/+* ECs within WT hosts is enhanced, suggesting that *Sema-PlxnD1* signaling acts prior to SeA sprouting. To investigate this possibility and determine its potential cellular basis we made *obd/+*-to-WT and WT-to-WT chimeras and plotted the distribution of donor ECs within the host's trunk vasculature shortly after SeA sprouts launch (Figure S2B). Consistent with *Sema-PlxnD1* signaling's dispensability for artery-vein differentiation (Torres-Vazquez et al., 2004) ECs from both donors contributed to the WT host's aorta equally. However, ECs from *obd/+* donors were enriched along the aorta's dorsal side (Figure 2F) and *obd* ECs also preferentially occupy this locale in WT hosts (Figures S1C and S2C). In contrast, ECs with a cell autonomous impairment in downstream VEGF signaling that abrogates SeA angiogenesis localize to the aorta's ventral side within WT hosts (Covassin et al., 2009).

The aorta's dorsal side lies near the trunk's paracrine sources of pro-angiogenic VEGF (Lawson et al., 2002) and is the aortic angiogenic region (Ahn et al., 2000; Wilkinson et al., 2009). Importantly, *obd/+* lacks aortic dorso-ventral polarization defects: both WT and *obd* display similar expression of the aortic dorsal side marker *tbx20* (data not shown) and make red blood cells, which derive from the aorta's ventral side (data not shown) (Wilkinson et al., 2009).

Hence, *Sema-PlxnD1* signaling plays a pre-sprouting role in SeA angiogenesis and the cellular basis for the enhanced angiogenic response of *obd/+* arterial ECs is, at least, related

to their ability to localize early within the WT host's aortic roof, a property likely due to increased VEGF responsiveness. Notably, in heterogenotypic chimeras *plxnd1* genetic dosage affects aortic cell distribution (Figure 2F) and tip cell positional status (Figure 2E) similarly but to different extents. Hence, Sema-PlxnD1 signaling likely exerts other pre-and/or post-sprouting effects, like modulating the angiogenic cell's launching schedule and/or positional persistence (Childs et al., 2002; Jakobsson et al., 2010; Kearney et al., 2004).

Sema-PlxnD1 signaling regulates the abundance of the VEGF antagonist encoded by soluble *flt1* (*sflt1*)

To determine the molecular mechanism by which Sema-PlxnD1 signaling represses angiogenic potential we used WISH (Moens, 2008) to visualize the expression of twelve components and targets of the VEGF and Notch signaling cascades, including artery-vein differentiation markers (see Supplemental Information). Only *flt1* (*fms-related tyrosine kinase/vegf receptor 1*) (Bussmann et al., 2007; Krueger et al., 2011) expression was visibly affected in *obd*. We found that zebrafish *flt1* pre-mRNA is alternatively spliced into transcripts encoding products similar to the soluble (sFlt1) and membrane (mFlt1) mammalian proteins that function as high-affinity VEGF decoys or receptor/co-receptor tyrosine kinases, respectively (Figure 3A–B) (Krueger et al., 2011; Rahimi, 2006). Using isoform-specific riboprobes we detected *sflt1* and *mflt1* transcripts in the WT trunk arterial tree at 21–28 hpf (Figure 3C–E) (Krueger et al., 2011). In contrast, *sflt1* was barely detectable in *obd* despite robust *mflt1* staining (Figure 3F–H), suggesting that Sema-PlxnD1 signaling modulates the relative abundance of *flt1* isoforms and/or *flt1* transcription. We used qPCR to compare the mRNA levels of WT and *obd/+*, which have identical EC abundances. We measured the transcript levels of both *flt1* isoforms and, separately, quantified the YFP mRNA output of the *flt1* transcriptional reporter *Tg(flt1:YFP)^{hu4624}* (Hogan et al., 2009a). *obd/+* shows reduced *sflt1* (four-fold) and increased *mflt1* (two-fold) levels, but unaltered *flt1* transcriptional levels (Figures 3I), and, confocal imaging reveals no clear differences in *Tg(flt1:YFP)^{hu4624}* expression between WT and *obd* (Figure S3C). Finally, ELISA-based measurements of FLT1 from extracts of HUVECs (human umbilical vein ECs) exposed to both VEGF and the canonical PlxnD1 ligand Sema3E reveal that shRNA-mediated *PLXND1* knockdown reduces FLT1 without decreasing *FLT1* transcription (Figure 3J and S3A, see also S3B).

We conclude that Sema-PlxnD1 signaling acts via a post-transcriptional mechanism to ensure *sflt1*'s proper abundance within the trunk's arterial tree and propose this model: *sflt1* acts as a PlxnD1 effector that antagonizes pro-angiogenic VEGF signaling to limit angiogenic potential.

Partial reduction of both *plxnd1* and *sflt1* enhances SeA angiogenesis

If the proposed model is true, *plxnd1* and *sflt1* should interact genetically to limit SeA angiogenesis. We tested this prediction with a morpholino (MO) (Morcos, 2007) that inhibits the alternative splicing event that yields *sflt1* (Figure S4A–B). The *sflt1*-splice MO induces aberrantly branched SeA sprouts in WT and *obd*-like SeA sprout defects such as ectopic launching and aberrant branching in *obd/+* heterozygotes (Figures 4B, D, E–F and S4C). Similarly, a pan-*flt1* splice-blocking MO (Rottbauer et al., 2005) targeting both *sflt1* and *mflt1* also induces *obd*-like SeA sprout defects in *obd/+* (Figure S4E–F). Of note, a different pan-*flt1* MO also induces SeA misbranching in WT (Krueger et al., 2011). Both the expressivity and penetrance of these abnormalities is greater in *sflt1*-splice than in pan-*flt1* morphants, likely due to differences in knockdown efficiencies and the combined effects of inactivating *flt1* isoforms with opposite roles (Figure 4F and S4F) (Rahimi, 2006). In contrast, WT and *obd/+* treated with mismatched control *sflt1* splice-blocking MO or an

mflt1-specific splice-blocking MO (Rottbauer et al., 2005) display normal SeA sprouts (Figure 4A, C, S4D, F).

These observations agree with the vascular organization roles of *plxnd1* (Gay et al., 2011) and *flt1* (Krueger et al., 2011; Rahimi, 2006), the differential activities of *flt1* isoforms (Chappell et al., 2009; Kappas et al., 2008; Rahimi, 2006) and *sflt1*'s low level in *obd*+ (Figure 3I). In short, *plxnd1* and *sflt1* (but not *mflt1*) interact genetically to modulate SeA sprout positioning, abundance and patterning.

Endothelial over-expression of *sflt1*, but not *mflt1*, inhibits SeA angiogenesis

Based on our model *sflt1*, like Sema-PlxnD1 signaling, should inhibit SeA angiogenesis. We tested this idea by over-expressing *sflt1* in an endothelial-specific fashion in both WT and *obd* via the GAL4/UAS system (Figure S4G). We found that *sflt1* over-expression suppresses SeA sprouting in WT and *obd* (Figure 4G–H"). To determine if *mflt1* plays similar vascular roles during SeA angiogenesis we analyzed the effects of *mflt1* over-expression. This treatment does not abrogate SeA sprouting but instead induces ectopic SeA sprouting at low frequency, consistent with the weak *mflt1* pro-angiogenic activity reported (Rahimi, 2006) (Figure S4H). Hence, within the trunk vasculature *sflt1* and *mflt1* play distinct roles, with *sflt1* acting as an inhibitor of SeA angiogenesis.

sflt1 inhibits SeA angiogenesis cell autonomously

Based on the model proposed, *sflt1*, like *plxnd1*, should act cell autonomously within the trunk's endothelium to suppress SeA angiogenesis. Given the lack of *flt1* mutants we tested this prediction by combining *sflt1* over-expression with cell transplantation experiments using donors and hosts carrying different endothelial reporters to distinguish ECs according to their genotype. We made chimeras to determine if over-expressed *sflt1* inhibits SeA sprouting non cell-autonomously. We transplanted *obd* cells into WT hosts with GAL4/UAS system-dependent mosaic endothelial co-expression of *sflt1* and fluorescent DsRed protein. We found that WT aortic ECs over-expressing *sflt1* (DsRed⁺) fail to form SeA sprouts. However, neighboring *obd* donor and WT host aortic ECs without *sflt1* over-expression (DsRed⁻) form SeA sprouts (Figure 4I–I'). In another experiment we transplanted cells from *obd* donors with endothelial *sflt1* over-expression (DsRed⁺) into WT hosts. While the *obd* aortic ECs with *sflt1* over-expression (DsRed⁺) failed to form SeA sprouts, neighboring WT and donor *obd* ECs not over-expressing *sflt1* (DsRed⁻) formed SeA sprouts (Figure S4I). Thus, *sflt1* acts cell autonomously despite the potential diffusible nature of its encoded product.

The exacerbated SeA angiogenesis of *obd* requires VEGF signaling

sflt1 encodes a VEGF signaling antagonist whose levels are greatly reduced in *obd* (Figure 3). To test if VEGF signaling is required for *obd*'s SeA angiogenesis we chemically inhibited VEGF receptor activation with SU5416 (Herbert et al., 2009). SU5416, but not its vehicle (DMSO), abrogates SeA sprouting in WT and *obd* (Figure 5A–B, E–F; see also Figure S5B). Similarly, MO-induced *vegfa* activity reduction also abrogates *obd*'s SeA angiogenesis (Childs et al., 2002). These findings indicate *obd*'s excessive SeA angiogenesis is VEGF-dependent.

VEGF signaling is enhanced in *obd*

The VEGF cascade splits downstream of the VEGF receptors into PLCG1 (*phospholipase C gamma1*; *plcg1*) and PI3K^{p110a} (phosphoinositide 3-kinase p110a isoform)-dependent pro-angiogenic branches (Figure 5M) (Covassin et al., 2009; Graupera et al., 2008). Our model predicts enhanced VEGF signaling in *obd*. Hence, angiogenic deficits due to impaired

VEGF signaling, such as those of *plcg1* mutants, should be ameliorated in an *obd* background. *plcg1* lacks SeA sprouts (Figure 5C) (Covassin et al., 2009). However, *obd; plcg1* double mutants show too many and ectopic SeA sprouts (Figure 5D and S5A) that express *flt4* and a trunk arterial tree with reduced *sflt1* abundance (data not shown). *obd; plcg1*'s SeA sprouting recovery requires VEGF signaling, since SU5416 suppresses it (Figure 5H). These observations support the notion that Sema-PlxnD1 cascade inactivation enhances VEGF signaling, suggesting that *obd; plcg1*'s angiogenic recovery is VEGF/PI3K^{P110}-dependent.

We tested this possibility via chemical inhibition of PI3K^{P110} activity with AS605240 (Herbert et al., 2009). PLCG function removal has a greater impact on angiogenesis than PI3K^{P110a} inactivation (Covassin et al., 2009; Graupera et al., 2008). Accordingly, AS605240 neither abrogates SeA angiogenesis in WT or *obd* nor ameliorates *plcg1*'s angiogenic deficit (Figure 5I–K). However, AS605240 blocks SeA sprouting in *obd; plcg1* (Figure 5L), indicating that pro-angiogenic VEGF/PI3K^{P110} activity is limiting under *plcg1*-deficient conditions. Hence, compared with *obd* (Figure 5B), *obd; plcg1* show fewer and stunted SeA sprouts that fail to form DLAVs (Figures 5D, 1D and 6L).

We further confirmed the link between Sema-PlxnD1 and VEGF signaling by observing that hypomorphic mutants of *kdrl*, which encodes the duplicate canonical VEGF pathway component VEGF receptor 2/VEGFR-2/KDR, show SeA angiogenic deficits (Covassin et al., 2009; Habeck et al., 2002) that are ameliorated in an *obd* background (Figure S5C).

To selectively determine Sema-PlxnD1 signaling's effect on VEGF-induced cellular responses we used a HUVEC proliferation assay (Figure 5N). We found that VEGF-induced HUVEC proliferation is reduced by Sema3E exposure and that the latter effect is abrogated via *PLXND1* (Bellon et al., 2010; Fukushima et al., 2011; Sakurai et al., 2010; Uesugi et al., 2009) or *FLT1* knockdown (Figure 5N and S5D). Accordingly, VEGF/Sema3E-treated HUVECs make less FLT1 protein upon *PLXND1* knockdown (Figure 3J). Of note, *PLXND1* knockdown in HUVECs does not affect *FLT1* transcription (Figure S5D), paralleling our *in vivo* data indicating that Sema-PlxnD1 signaling modulates *sflt1* abundance post-transcriptionally (Figures 3C–I and S3C).

WISHs suggest that *sflt1*'s level in the trunk's arterial tree is independent of VEGF signaling: SU5416 treatment does not reduce *sflt1* abundance in WT nor increases it in *obd* (Figure S5B). Hence, *obd*'s decreased *sflt1* abundance is not secondary to enhanced VEGF signaling but rather at least one of its causes.

Sema-PlxnD1 and Notch signaling play distinct and additive roles in SeA angiogenesis

Notch signaling also negatively regulates SeA sprouting (Leslie et al., 2007; Siekmann and Lawson, 2007). We thus compared the arterial tree phenotypes induced by loss of Sema-PlxnD1 and Notch signaling. We found that unlike *obd*, SeA sprout abundance and distribution are normal in *mind bomb (mib)* mutants, in which a ubiquitin ligase required for Notch signaling is inactive (Figure S6A) (Itoh et al., 2003; Lawson et al., 2002; Lawson and Weinstein, 2002). Likewise, Notch pathway inactivation via mutations in either *mib* or *delta-like ligand 4 (dll4)*, which encodes a Notch ligand expressed in the trunk's arterial tree (Leslie et al., 2007), fails to ameliorate the angiogenic deficit of *plcg1* (Figure S6C).

Studies in other systems and/or vascular beds suggest Notch signaling promotes *flt1* expression (Bussmann et al., 2011; del Toro et al., 2010; Funahashi et al., 2010; Harrington et al., 2008; Jakobsson et al., 2010; Suchting et al., 2007), prompting us to ask if Notch signaling is reduced in *obd* or modulates the trunk's arterial tree expression of *flt1* and its isoforms.

WISH expression analysis of Notch pathway components (*deltac*, *dll4 notch5* and *gridlock*) and targets (*gridlock*, *ephrin-B2a*, *flt4* and *ephB4a*) fails to uncover evidence for reduced Notch signaling in *obd* (data not shown) and, endothelial expression of the transgenic Notch signaling reporters *Tg(Tp1bglob:hmgbl-mCherry)^{jh11}* and *Tg(Tp1bglob:eGFP)^{um14}* (Nicoli et al., 2010; Parsons et al., 2009) is similar in WT and *obd* (Figure 6A–B and data not shown), consistent with the notion that in *obd* Notch activity is preserved.

Visual comparison of the *flt1* transcriptional reporter expression (Hogan et al., 2009a; Hogan et al., 2009b) in WT, *obd* mutants and *mib* morphants (Figure S3C) reveals no significant differences. *Tg(flt1:YFP)^{hu4624}* expression is also unaffected in *dll4* morphants (Geudens et al., 2010). Moreover, WISH of *mib* mutants reveals no visible reduction in *sflt1* or *mflt1* abundance but rather a mild enhancement in *sflt1* and *mflt1* venous expression (Figure S6B). Consistent with the role of Notch signaling in artery/vein differentiation and angiogenesis, *mib* displays ectopic aortic *flt4* expression (Figure S6A) (Lawson et al., 2001; Siekmann and Lawson, 2007).

To elucidate the relationship between Sema-PlxnD1 and Notch signaling we analyzed the anatomical, cellular and molecular vascular phenotypes of *obd*; *mib* and the combined impact of inactivating both pathways on *plcg1*'s SeA angiogenesis deficit. We found that within the arterial tree *obd*; *mib* show *obd*-like SeA anatomical organization and *sflt1* abundance (Figure 6C–D) but *mib*-like *flt4* and *mflt1* expression patterns (Figure 6E–F). This mix of *obd*- and *mib*-like phenotypes reveals that Sema-PlxnD1 and Notch signaling play distinct vascular roles.

Yet we also find additive genetic interactions between both pathways: *obd*; *mib* have greater angiogenic cell abundance than *obd* or *mib* (Figure 6G–I) (Leslie et al., 2007; Siekmann and Lawson, 2007). Likewise, silencing *mib* (Itoh et al., 2003) in *obd*; *plcg* further increases their SeA sprout abundance (Figure 6J–L). Hence, in this sensitized background Notch signaling seems to play a minor role as a negative regulator of SeA sprout abundance, consistent with the loss of SeA sprouting induced by over-expression of constitutive-active Notch forms, the complex interplay between VEGF and Notch signaling and the lateral inhibition role of the latter (Jakobsson et al., 2010; Roca and Adams, 2007; Siekmann and Lawson, 2007). While these additive interactions suggest that Sema-PlxnD1 and Notch signaling modulate common aspects of angiogenic development, these pathways clearly make qualitatively and quantitatively different contributions via molecularly distinct mechanisms. For example, while both pathways antagonize VEGF signaling, they modulate different pathway components, namely *sflt1* and *flt4*. Together, these observations indicate that Notch signaling remains active in *obd* and that Sema-PlxnD1 signaling functions without Notch activity (Figure 7A), underscoring the distinct roles of Sema-PlxnD1 and Notch signaling in SeA angiogenesis.

DISCUSSION

Our findings reveal that Sema-PlxnD1 signaling acts as a pre-sprouting repressor of angiogenic potential in the trunk's arterial tree. We posit that Sema-PlxnD1 signaling fulfills this role, at least in part, by maintaining *sflt1*'s proper endothelial abundance to antagonize pro-angiogenic VEGF signaling (Figure 7A). We propose that the somitic *sema3a* and endothelial *plxnD1* expression preceding SeA sprouting (Torres-Vazquez et al., 2004) (Figure 7B) reproducibly yield differences in Sema-PlxnD1 signaling level, and thus in *sflt1* abundance, along the aorta (Figure 7C). Although the proposed variation in WT *sflt1* aortic levels appears beyond the resolution of WISH, we find that ECs from *obd*/+ donors (which have less *sflt1*) are more likely to become angiogenic in WT hosts. Indeed, ECs with the

lowest *Flt1* abundance make the angiogenic sprouts of WT and *Flt1^{lacZ/+}* mouse retinas and ES cell-derived vessels (Chappell et al., 2009).

Our WISH and qPCR data indicates that loss or reduction of Sema-PlxnD1 signaling leads to low *sflt1* abundance within both the aorta and SeA sprouts. Accordingly, our cell transplants show that Sema-PlxnD1 signaling acts cell autonomously to spatially restrict the aorta's angiogenic capacity (Figure 7D) and limit the angiogenic responses of ECs within SeA sprouts (Figure 7E).

While sFlt1 can act non-cell autonomously (Ambati et al., 2006); (Chappell et al., 2009; Kearney et al., 2004), its effective range is context-dependent (Goldman et al., 1998; James et al., 2009; Kendall and Thomas, 1993). In the trunk's arterial tree the anti-angiogenic effects of endothelial-specific *sflt1* over-expression appear cell autonomous. sFlt1 forms VEGF-bridged inhibitory complexes with the pro-angiogenic receptors Flk1/Kdr (Bussmann et al., 2008; Kendall et al., 1996) and mFlt1 (Kendall and Thomas, 1993) and binds to the endothelial extracellular matrix, which abundantly surrounds the aorta (Jin et al., 2005; Orecchia et al., 2003), both observations suggest how sFlt1's effective range might be limited within the aorta. Alternatively, sFlt1 might act in an intracrine manner, as proposed for mFlt1 (Lee et al., 2007b).

Our model implies that PlxnD1 signaling in response to paracrine Sema3 cues is key for the proper spatial modulation of angiogenic capacity within the aorta (Gay et al., 2011). Yet our findings do not rule out the potential involvement of autocrine Sema3 cues in PlxnD1 signaling prior to and/or during SeA sprouting (Banu et al., 2006; Kutschera et al., 2011; Lamont et al., 2009; Serini et al., 2003; Toyofuku et al., 2007). Similarly, endothelial Sema-PlxnD1 signaling could impact the pro-angiogenic activity of both paracrine and autocrine VEGFs (Childs et al., 2002; Covassin et al., 2006; da Silva et al., 2010; Hogan et al., 2009b; Lee et al., 2007a; Siekmann and Lawson, 2007; Tammela et al., 2008).

Our study reveals a key mechanistic link between Sema-PlxnD1 and VEGF signaling (Bellon et al., 2010; Fukushima et al., 2011; Sakurai et al., 2010; Uesugi et al., 2009). Consistent with defects in exon selection during *flt1*'s alternative splicing and/or alterations in the mRNA stability of *flt1* isoforms, impaired Sema-PlxnD1 signaling leads to contrasting post-transcriptional changes in *sflt1* and *mflt1* abundance. Sema-PlxnD1 signaling inactivates Ras-related proteins, antagonizes integrin and PI3K signaling and modulates cytoskeletal dynamics (Gay et al., 2011). How these PlxnD1-mediated events are connected to *flt1*'s post-transcriptional regulation and angiogenesis will be addressed by future studies.

Here we show that Sema-PlxnD1 and Notch signaling can function independently of each other and play largely distinct cellular and molecular roles. However, Sema-PlxnD1 activity antagonizes VEGF responsiveness and Notch and VEGF signaling are linked by complex feedback loops (Jakobsson et al., 2009; Lobov et al., 2007; Williams et al., 2006). Hence, we anticipate functional interactions between both pathways via the VEGF cascade. For example, it is likely that the enhanced VEGF signaling of ECs with less Sema-PlxnD1 activity allows them to exert a stronger Dll4/Notch-mediated lateral inhibition upon their neighbors, enabling the former to more often become angiogenic and/or, acquire and/or keep a tip cell positional status (Jakobsson et al., 2010; Leslie et al., 2007; Siekmann and Lawson, 2007). Remarkably, the combined loss of both Sema-PlxnD1 (*plxnd1*) and Notch signaling (*mib*) signaling does not enable every aortic EC to sprout, suggesting that other pathways and/or mechanisms limit the trunk's arterial tree angiogenic capacity.

Together with prior studies (Gay et al., 2011), our findings indicate that Sema-PlxnD1 signaling regulates distinct yet interconnected aspects of angiogenic development: the spatial allocation of angiogenic capabilities and the guidance of growing sprouts. It is likely

that these roles, and their bases, are evolutionarily conserved (see (Gay et al., 2011)). Changes in *sflt1* abundance induce congenital vascular malformations (Acevedo and Cheresh, 2008), gestational hypertension (Rahimi, 2006) and are associated with cancer (Aref et al., 2005). Hence, mutations and polymorphisms that affect Sema-PlxnD1 signaling are likely modifiers of these diseases. Conversely, alterations in *sflt1* abundance and/or activity might impact Sema-PlxnD1 signaling dependent processes like cardiovascular and nervous system development and both tumor angiogenesis and metastasis (Gay et al., 2011; Raab and Plate, 2007; Takahashi and Shibuya, 2005). Overall, the regulation of *sflt1* abundance via Sema-PlxnD1 signaling has broad biomedical implications beyond angiogenesis and provides a new way of understanding how Sema and VEGF signals might be integrated in many contexts.

EXPERIMENTAL PROCEDURES

Zebrafish

Embryos and adults kept and handled using standard laboratory conditions under New York University IACUC guidelines. Zebrafish stocks and genotyping methods/reagents described in the Supplemental Information.

Imaging

Live and fluorescently immunostained embryos imaged via confocal microscopy, whole mount RNA *in situ* hybridized embryos and drug treated animals imaged via transmitted light microscopy. All embryos mounted sideways. Details in the Supplemental Information.

SeA sprout abundance and position quantification

Quantifications done using confocal images of immunofluorescently stained 23 hpf *Tg(fli:EGFP)^{y1}* embryos. SeA sprouts: individual EGFP-positive aortic dorsal projections that reach or surpass the Horizontal Myoseptum (HM; see Figure 1). SeA sprout positions: Correct (SeA base abuts directly the anterior side of neighboring somite boundary), ectopic (all other base locations). SeA sprouts were counted in four adjacent anterior trunk segments and averaged to yield a SeA sprouts/somite boundary ratio. Student's t-test (homocedastic, two-tail distribution) was used to analyze the differences between the means of cell number data sets.

Endothelial cell abundance quantification

21, 23 and 32 hpf *Tg(fli:nEGFP)^{y7}*; *Tg(flk1:ras-mCherry)^{s896}* and *Tg(flk1:EGFP-NLS)*; *Tg(flk1:ras-mCherry)^{s896}* immunofluorescently stained embryos were used to visualize EC nuclei and vascular anatomy. Confocal sections across the width of the anterior trunk were collected and 3D-projected with Imaris 6.2.1 software (Bitplane AG). EGFP-positive nuclei were marked (measurement point application) and counted. Since WT SeAs launch next to somite boundaries (SBs) but *obd* SeAs arise from these and other sites we divided the trunk vasculature into segments delimited by the posterior and anterior halves of consecutive bilateral somite pairs and counted EC nuclei within each segment. Based on their location, EC nuclei were assigned to the axial vessels (AxV; aorta and vein), the SeAs and/or DLAVs. AxV (rather than aortic- and venous-specific) EC abundance was scored since the aorta and vein are not fully distinct at 21 and 23 hpf (Herbert et al., 2009). We counted ECs in three consecutive trunk segments (located dorsal to the yolk extension) and averaged them to obtain ECs/bilateral somite pair ratios for each location. Student's t-test (homocedastic, two-tail distribution) was used to analyze the differences between the means of EC number data sets. Note: Not every EC whose nucleus is labeled by *Tg(fli:nEGFP)^{y7}*

(green) is marked by *Tg(flkl:ras-mCherry)^{s896}* (red) due to the latter's expression mosaicism (Figure S1A).

Cell transplants

Cell transplants done with 3–4 hpf donor and host blastula-stage embryos as in (Carmany-Rampey and Moens, 2006). 30–50 cells were aspirated from the donor's animal pole and placed into the host's lateral margin zone. Donors and hosts carried distinct endothelial-specific reporters to easily identify the source of ECs within chimeras. *plxnd1*'s cell autonomy: We used both WT and *obd* as *Tg(fli:EGFP)^{y1}* donors and as *Tg(flkl:ras-mcherry)^{s896}* hosts. 1 nl of a 5% solution of lineage tracer (dextran Alexa Fluor 647; Invitrogen) was injected into 1-cell stage donors. Chimeras fixed at 32 hpf. Quantification of mosaic SeA sprouts with tip cells of donor origin: We used both WT and *obd/+* as *Tg(fli:EGFP)^{y1}* donors and as *Tg(flkl:ras-mcherry)^{s896}* hosts. Chimeras fixed at 28 hpf. Quantification of the distribution of ECs of donor origin within the trunk vasculature of chimeras: We used both WT and *obd/+* as *Tg(flkl:EGFP-NLS)* donors. *Tg(flkl:ras-mcherry)^{s896}* used as hosts. Chimeras fixed at 21–23 hpf. Embryos with ECs of donor origin within the trunk's vascular tree were selected. Confocal images of their whole trunk vasculature were taken and analyzed as described in Figure S2B. *sflt1*'s cell autonomy: We used *Tg(fli:EGFP)^{y1}* donors and *Tg(flkl:EGFP-NLS)* hosts. Endothelial-specific, *sflt1* mosaic over-expression in donors or hosts done using the *Tg(fli:gal4ff)^{ubs4}* GAL4 driver line and the bidirectional *UAS* vector *pTol[DsRed::UAS::sflt1]*.

Whole mount RNA *in situ* hybridization (WISH)

WISH performed as in (Moens, 2008). The list of analyzed genes and riboprobe synthesis protocols are in the Supplemental Experimental Procedures.

Morpholino oligo (MO) injection

MOs (Gene Tools, LLC) were injected into 1-cell stage *Tg(fli:EGFP)^{y1}* embryos as in (Morcos, 2007). MO sequences and validation methods are in the Supplemental Experimental Procedures.

Drug treatments

Embryos were dechorionated before treatment. Treatments began at 16 (Figure 5A–L) or 20 hpf (Figure S5B; to prevent the dramatic aortic size reduction induced by earlier treatments). Control embryos were treated with 0.025% dimethyl sulfoxide (DMSO; Sigma) in water. Inhibitor-treated embryos were incubated in 0.25 μ M AS605240 or 0.5 μ M SU5416 (Sigma) aqueous solutions of 0.025% DMSO.

Quantitative real time polymerase chain reaction (qPCR)

Total mRNA (zebrafish embryos) and RNA (HUVECs) extraction and cDNA synthesis done as per Supplementary Experimental Procedures. qPCR DNA products amplified with Power SYBR Green 2X Master Mix (Applied Biosystems) as per manufacturer's instructions. Whole embryo qPCR products were quantified with a 7900HT Real-Time PCR System (Applied Biosystems). Relative *sflt1*, *mflt1* and *YFP* mRNA levels normalized to *bactin2* transcript abundance. For shRNA control experiments, products were quantified with a PRISM 7900 (Applied Biosystems). Relative *PLXND1* and *FLT1* levels normalized to *glyceraldehyde-3-phosphate (GAPDH)* abundance. Primer sequences are in the Supplemental Experimental Procedures.

Supplementary Material

Refer to Web version on PubMed Central for supplementary material.

Acknowledgments

We thank N.C. Chi, C-B. Chien, S. Childs, A. Chitnis, S.L. Johnson, K. Kawakami, N.D. Lawson, M. Parsons, S. Schulte-Merker, D. Stainier, B.M. Weinstein, and the Zebrafish International Resource Center for reagents; G. Fishell, E.J.A. Hubbard, H. Knaut, J.F. Nance, D.B. Rifkin, K.L. Targoff, J.E. Treisman, S.R. Schwab, F. Ulrich, K.A. Yaniv and D. Yelon for discussions; J. Zavadil (NYU Cancer Institute Genomics Facility), D. Dalfo and J-Y. Roignant for qPCR advice; D. Chan for administrative help. Support: A.K. (Werner Siemens-Foundation; Switzerland), C.M.G. (NICHD Training Program Grant 5T32HD007520-05), J.T-V (The David Himelberg Foundation and NHLBI). We apologize to authors not cited due to limited space.

References

- Acevedo LM, Cheresch DA. Suppressing NFAT increases VEGF signaling in hemangiomas. *Cancer Cell*. 2008; 14:429–430. [PubMed: 19061833]
- Ahn DG, Ruvinsky I, Oates AC, Silver LM, Ho RK. *tbx20*, a new vertebrate T-box gene expressed in the cranial motor neurons and developing cardiovascular structures in zebrafish. *Mech Dev*. 2000; 95:253–258. [PubMed: 10906473]
- Ambati BK, Nozaki M, Singh N, Takeda A, Jani PD, Suthar T, Albuquerque RJ, Richter E, Sakurai E, Newcomb MT, et al. Corneal avascularity is due to soluble VEGF receptor-1. *Nature*. 2006; 443:993–997. [PubMed: 17051153]
- Aref S, El Sherbiny M, Goda T, Fouda M, Al Askalany H, Abdalla D. Soluble VEGF/sFlt1 ratio is an independent predictor of AML patient out come. *Hematology*. 2005; 10:131–134. [PubMed: 16019458]
- Banu N, Teichman J, Dunlap-Brown M, Villegas G, Tufro A. Semaphorin 3C regulates endothelial cell function by increasing integrin activity. *FASEB J*. 2006; 20:2150–2152. [PubMed: 16940438]
- Bellon A, Luchino J, Haigh K, Rougon G, Haigh J, Chauvet S, Mann F. VEGFR2 (KDR/Flk1) signaling mediates axon growth in response to semaphorin 3E in the developing brain. *Neuron*. 2010; 66:205–219. [PubMed: 20434998]
- Bussmann J, Bakkers J, Schulte-Merker S. Early endocardial morphogenesis requires *Scf/Tal1*. *PLoS Genet*. 2007; 3:e140. [PubMed: 17722983]
- Bussmann J, Lawson N, Zon L, Schulte-Merker S. Zebrafish VEGF receptors: a guideline to nomenclature. *PLoS Genet*. 2008; 4:e1000064. [PubMed: 18516225]
- Bussmann J, Wolfe SA, Siekmann AF. Arterial-venous network formation during brain vascularization involves hemodynamic regulation of chemokine signaling. *Development*. 2011; 138:1717–1726. [PubMed: 21429983]
- Carmany-Rampey A, Moens CB. Modern mosaic analysis in the zebrafish. *Methods*. 2006; 39:228–238. [PubMed: 16829130]
- Carmeliet P. Angiogenesis in life, disease and medicine. *Nature*. 2005; 438:932–936. [PubMed: 16355210]
- Chappell JC, Taylor SM, Ferrara N, Bautch VL. Local guidance of emerging vessel sprouts requires soluble Flt-1. *Dev Cell*. 2009; 17:377–386. [PubMed: 19758562]
- Childs S, Chen JN, Garrity DM, Fishman MC. Patterning of angiogenesis in the zebrafish embryo. *Development*. 2002; 129:973–982. [PubMed: 11861480]
- Covassin LD, Siekmann AF, Kacergis MC, Laver E, Moore JC, Villefranc JA, Weinstein BM, Lawson ND. A genetic screen for vascular mutants in zebrafish reveals dynamic roles for *Vegf/Plcg1* signaling during artery development. *Dev Biol*. 2009; 329:212–226. [PubMed: 19269286]
- Covassin LD, Villefranc JA, Kacergis MC, Weinstein BM, Lawson ND. Distinct genetic interactions between multiple *Vegf* receptors are required for development of different blood vessel types in zebrafish. *Proc Natl Acad Sci U S A*. 2006; 103:6554–6559. [PubMed: 16617120]
- da Silva RG, Tavora B, Robinson SD, Reynolds LE, Szekeres C, Lamar J, Batista S, Kostourou V, Germain MA, Reynolds AR, et al. Endothelial alpha3beta1-integrin represses pathological

- angiogenesis and sustains endothelial-VEGF. *Am J Pathol.* 2010; 177:1534–1548. [PubMed: 20639457]
- De Bock K, De Smet F, Leite De Oliveira R, Anthonis K, Carmeliet P. Endothelial oxygen sensors regulate tumor vessel abnormalization by instructing phalanx endothelial cells. *J Mol Med.* 2009; 87:561–569. [PubMed: 19455291]
- del Toro R, Prahst C, Mathivet T, Siegfried G, Kaminker JS, Larrivee B, Breant C, Duarte A, Takakura N, Fukamizu A, et al. Identification and functional analysis of endothelial tip cell-enriched genes. *Blood.* 2010; 116:4025–4033. [PubMed: 20705756]
- Fukushima Y, Okada M, Kataoka H, Hirashima M, Yoshida Y, Mann F, Gomi F, Nishida K, Nishikawa S, Uemura A. *Sema3E-PlexinD1* signaling selectively suppresses disoriented angiogenesis in ischemic retinopathy in mice. *J Clin Invest.* 2011; 121:1974–1985. [PubMed: 21505259]
- Funahashi Y, Shawber CJ, Vorontchikhina M, Sharma A, Outtz HH, Kitajewski J. Notch regulates the angiogenic response via induction of VEGFR-1. *J Angiogenes Res.* 2010; 2:3. [PubMed: 20298529]
- Gay CM, Zygmunt T, Torres-Vazquez J. Diverse functions for the semaphorin receptor PlexinD1 in development and disease. *Dev Biol.* 2011; 349:1–19. [PubMed: 20880496]
- Geudens I, Herpers R, Hermans K, Segura I, Ruiz de Almodovar C, Bussmann J, De Smet F, Vandeveldel W, Hogan BM, Siekmann A, et al. Role of delta-like-4/Notch in the formation and wiring of the lymphatic network in zebrafish. *Arterioscler Thromb Vasc Biol.* 2010; 30:1695–1702. [PubMed: 20466977]
- Goldman CK, Kendall RL, Cabrera G, Soroceanu L, Heike Y, Gillespie GY, Siegal GP, Mao X, Bett AJ, Huckle WR, et al. Paracrine expression of a native soluble vascular endothelial growth factor receptor inhibits tumor growth, metastasis, and mortality rate. *Proc Natl Acad Sci U S A.* 1998; 95:8795–8800. [PubMed: 9671758]
- Graupera M, Guillermet-Guibert J, Foukas LC, Phng LK, Cain RJ, Salpekar A, Pearce W, Meek S, Millan J, Cutillas PR, et al. Angiogenesis selectively requires the p110alpha isoform of PI3K to control endothelial cell migration. *Nature.* 2008; 453:662–666. [PubMed: 18449193]
- Habeck H, Odenthal J, Walderich B, Maischein H, Schulte-Merker S. Analysis of a zebrafish VEGF receptor mutant reveals specific disruption of angiogenesis. *Curr Biol.* 2002; 12:1405–1412. [PubMed: 12194822]
- Harrington LS, Sainson RC, Williams CK, Taylor JM, Shi W, Li JL, Harris AL. Regulation of multiple angiogenic pathways by Dll4 and Notch in human umbilical vein endothelial cells. *Microvasc Res.* 2008; 75:144–154. [PubMed: 17692341]
- Herbert SP, Huiskens J, Kim TN, Feldman ME, Houseman BT, Wang RA, Shokat KM, Stainier DY. Arterial-venous segregation by selective cell sprouting: an alternative mode of blood vessel formation. *Science.* 2009; 326:294–298. [PubMed: 19815777]
- Hogan BM, Bos FL, Bussmann J, Witte M, Chi NC, Duckers HJ, Schulte-Merker S. *Ccbe1* is required for embryonic lymphangiogenesis and venous sprouting. *Nat Genet.* 2009a; 41:396–398. [PubMed: 19287381]
- Hogan BM, Herpers R, Witte M, Helotera H, Alitalo K, Duckers HJ, Schulte-Merker S. *Vegfc/Flt4* signalling is suppressed by Dll4 in developing zebrafish intersegmental arteries. *Development.* 2009b; 136:4001–4009. [PubMed: 19906867]
- Isogai S, Horiguchi M, Weinstein BM. The vascular anatomy of the developing zebrafish: an atlas of embryonic and early larval development. *Dev Biol.* 2001; 230:278–301. [PubMed: 11161578]
- Isogai S, Lawson ND, Torrealday S, Horiguchi M, Weinstein BM. Angiogenic network formation in the developing vertebrate trunk. *Development.* 2003; 130:5281–5290. [PubMed: 12954720]
- Itoh M, Kim CH, Palardy G, Oda T, Jiang YJ, Maust D, Yeo SY, Lorick K, Wright GJ, Ariza-McNaughton L, et al. Mind bomb is a ubiquitin ligase that is essential for efficient activation of Notch signaling by Delta. *Dev Cell.* 2003; 4:67–82. [PubMed: 12530964]
- Jakobsson L, Bentley K, Gerhardt H. VEGFRs and Notch: a dynamic collaboration in vascular patterning. *Biochem Soc Trans.* 2009; 37:1233–1236. [PubMed: 19909253]

- Jakobsson L, Franco CA, Bentley K, Collins RT, Ponsioen B, Aspalter IM, Rosewell I, Busse M, Thurston G, Medvinsky A, et al. Endothelial cells dynamically compete for the tip cell position during angiogenic sprouting. *Nat Cell Biol.* 2010; 12:943–953. [PubMed: 20871601]
- James JM, Gewolb C, Bautch VL. Neurovascular development uses VEGF-A signaling to regulate blood vessel ingression into the neural tube. *Development.* 2009; 136:833–841. [PubMed: 19176586]
- Jin SW, Beis D, Mitchell T, Chen JN, Stainier DY. Cellular and molecular analyses of vascular tube and lumen formation in zebrafish. *Development.* 2005; 132:5199–5209. [PubMed: 16251212]
- Kappas NC, Zeng G, Chappell JC, Kearney JB, Hazarika S, Kallianos KG, Patterson C, Annex BH, Bautch VL. The VEGF receptor Flt-1 spatially modulates Flk-1 signaling and blood vessel branching. *J Cell Biol.* 2008; 181:847–858. [PubMed: 18504303]
- Kearney JB, Kappas NC, Ellerstrom C, DiPaola FW, Bautch VL. The VEGF receptor flt-1 (VEGFR-1) is a positive modulator of vascular sprout formation and branching morphogenesis. *Blood.* 2004; 103:4527–4535. [PubMed: 14982871]
- Kendall RL, Thomas KA. Inhibition of vascular endothelial cell growth factor activity by an endogenously encoded soluble receptor. *Proc Natl Acad Sci U S A.* 1993; 90:10705–10709. [PubMed: 8248162]
- Kendall RL, Wang G, Thomas KA. Identification of a natural soluble form of the vascular endothelial growth factor receptor, FLT-1, and its heterodimerization with KDR. *Biochem Biophys Res Commun.* 1996; 226:324–328. [PubMed: 8806634]
- Krueger J, Liu D, Scholz K, Zimmer A, Shi Y, Klein C, Siekmann A, Schulte-Merker S, Cudmore M, Ahmed A, et al. Flt1 acts as a negative regulator of tip cell formation and branching morphogenesis in the zebrafish embryo. *Development.* 2011; 138:2111–2120. [PubMed: 21521739]
- Kutschera S, Weber H, Weick A, De Smet F, Genove G, Takemoto M, Prahst C, Riedel M, Mikelis C, Baulande S, et al. Differential endothelial transcriptomics identifies semaphorin 3G as a vascular class 3 semaphorin. *Arterioscler Thromb Vasc Biol.* 2011; 31:151–159. [PubMed: 20947821]
- Lamont RE, Lamont EJ, Childs SJ. Antagonistic interactions among Plexins regulate the timing of intersegmental vessel formation. *Dev Biol.* 2009; 331:199–209. [PubMed: 19422817]
- Larson JD, Wadman SA, Chen E, Kerley L, Clark KJ, Eide M, Lippert S, Nasevicius A, Ekker SC, Hackett PB, et al. Expression of VE-cadherin in zebrafish embryos: a new tool to evaluate vascular development. *Dev Dyn.* 2004; 231:204–213. [PubMed: 15305301]
- Lawson ND, Scheer N, Pham VN, Kim CH, Chitnis AB, Campos-Ortega JA, Weinstein BM. Notch signaling is required for arterial-venous differentiation during embryonic vascular development. *Development.* 2001; 128:3675–3683. [PubMed: 11585794]
- Lawson ND, Vogel AM, Weinstein BM. sonic hedgehog and vascular endothelial growth factor act upstream of the Notch pathway during arterial endothelial differentiation. *Dev Cell.* 2002; 3:127–136. [PubMed: 12110173]
- Lawson ND, Weinstein BM. In vivo imaging of embryonic vascular development using transgenic zebrafish. *Dev Biol.* 2002; 248:307–318. [PubMed: 12167406]
- Lee S, Chen TT, Barber CL, Jordan MC, Murdock J, Desai S, Ferrara N, Nagy A, Roos KP, Iruela-Arispe ML. Autocrine VEGF signaling is required for vascular homeostasis. *Cell.* 2007a; 130:691–703. [PubMed: 17719546]
- Lee TH, Seng S, Sekine M, Hinton C, Fu Y, Avraham HK, Avraham S. Vascular endothelial growth factor mediates intracrine survival in human breast carcinoma cells through internally expressed VEGFR1/FLT1. *PLoS Med.* 2007b; 4:e186. [PubMed: 17550303]
- Leslie JD, Ariza-McNaughton L, Bermange AL, McAdow R, Johnson SL, Lewis J. Endothelial signalling by the Notch ligand Delta-like 4 restricts angiogenesis. *Development.* 2007; 134:839–844. [PubMed: 17251261]
- Lobov IB, Renard RA, Papadopoulos N, Gale NW, Thurston G, Yancopoulos GD, Wiegand SJ. Delta-like ligand 4 (Dll4) is induced by VEGF as a negative regulator of angiogenic sprouting. *Proc Natl Acad Sci U S A.* 2007; 104:3219–3224. [PubMed: 17296940]
- Moens, C. Cold Spring Harb Protoc. 2008. Whole Mount RNA In Situ Hybridization on Zebrafish Embryos.

- Morcos PA. Achieving targeted and quantifiable alteration of mRNA splicing with Morpholino oligos. *Biochem Biophys Res Commun.* 2007; 358:521–527. [PubMed: 17493584]
- Nicoli S, Standley C, Walker P, Hurlstone A, Fogarty KE, Lawson ND. MicroRNA-mediated integration of haemodynamics and Vegf signalling during angiogenesis. *Nature.* 2010; 464:1196–1200. [PubMed: 20364122]
- Orecchia A, Lacal PM, Schietroma C, Morea V, Zambruno G, Failla CM. Vascular endothelial growth factor receptor-1 is deposited in the extracellular matrix by endothelial cells and is a ligand for the alpha 5 beta 1 integrin. *J Cell Sci.* 2003; 116:3479–3489. [PubMed: 12865438]
- Parsons MJ, Pisharath H, Yusuff S, Moore JC, Siekmann AF, Lawson N, Leach SD. Notch-responsive cells initiate the secondary transition in larval zebrafish pancreas. *Mech Dev.* 2009; 126:898–912. [PubMed: 19595765]
- Phng LK, Gerhardt H. Angiogenesis: a team effort coordinated by notch. *Dev Cell.* 2009; 16:196–208. [PubMed: 19217422]
- Phng LK, Potente M, Leslie JD, Babbage J, Nyqvist D, Lobov I, Ondr JK, Rao S, Lang RA, Thurston G, et al. Nrarp coordinates endothelial Notch and Wnt signaling to control vessel density in angiogenesis. *Dev Cell.* 2009; 16:70–82. [PubMed: 19154719]
- Raab S, Plate KH. Different networks, common growth factors: shared growth factors and receptors of the vascular and the nervous system. *Acta Neuropathol.* 2007; 113:607–626. [PubMed: 17492293]
- Rahimi N. VEGFR-1 and VEGFR-2: two non-identical twins with a unique physiognomy. *Front Biosci.* 2006; 11:818–829. [PubMed: 16146773]
- Roca C, Adams RH. Regulation of vascular morphogenesis by Notch signaling. *Genes Dev.* 2007; 21:2511–2524. [PubMed: 17938237]
- Roos M, Schachner M, Bernhardt RR. Zebrafish semaphorin Z1b inhibits growing motor axons in vivo. *Mech Dev.* 1999; 87:103–117. [PubMed: 10495275]
- Rottbauer W, Just S, Wessels G, Trano N, Most P, Katus HA, Fishman MC. VEGF-PLCgamma1 pathway controls cardiac contractility in the embryonic heart. *Genes Dev.* 2005; 19:1624–1634. [PubMed: 15998812]
- Sakurai A, Gavard J, Annas-Linhares Y, Basile JR, Amornphimoltham P, Palmby TR, Yagi H, Zhang F, Randazzo PA, Li X, et al. Semaphorin 3E initiates antiangiogenic signaling through plexin D1 by regulating Arf6 and R-Ras. *Mol Cell Biol.* 2010; 30:3086–3098. [PubMed: 20385769]
- Serini G, Valdembrì D, Zanivan S, Morterra G, Burkhardt C, Caccavari F, Zammataro L, Primo L, Tamagnone L, Logan M, et al. Class 3 semaphorins control vascular morphogenesis by inhibiting integrin function. *Nature.* 2003; 424:391–397. [PubMed: 12879061]
- Siekmann AF, Covassin L, Lawson ND. Modulation of VEGF signalling output by the Notch pathway. *Bioessays.* 2008; 30:303–313. [PubMed: 18348190]
- Siekmann AF, Lawson ND. Notch signalling limits angiogenic cell behaviour in developing zebrafish arteries. *Nature.* 2007; 445:781–784. [PubMed: 17259972]
- Suchting S, Freitas C, le Noble F, Bedito R, Breant C, Duarte A, Eichmann A. The Notch ligand Delta-like 4 negatively regulates endothelial tip cell formation and vessel branching. *Proc Natl Acad Sci U S A.* 2007; 104:3225–3230. [PubMed: 17296941]
- Takahashi H, Shibuya M. The vascular endothelial growth factor (VEGF)/VEGF receptor system and its role under physiological and pathological conditions. *Clin Sci (Lond).* 2005; 109:227–241. [PubMed: 16104843]
- Tammela T, Zarkada G, Wallgard E, Murtomaki A, Suchting S, Wirzenius M, Waltari M, Hellstrom M, Schomber T, Peltonen R, et al. Blocking VEGFR-3 suppresses angiogenic sprouting and vascular network formation. *Nature.* 2008; 454:656–660. [PubMed: 18594512]
- Torres-Vazquez J, Gitler AD, Fraser SD, Berk JD, Van NP, Fishman MC, Childs S, Epstein JA, Weinstein BM. Semaphorin-plexin signaling guides patterning of the developing vasculature. *Dev Cell.* 2004; 7:117–123. [PubMed: 15239959]
- Toyofuku T, Yabuki M, Kamei J, Kamei M, Makino N, Kumanogoh A, Hori M. Semaphorin-4A, an activator for T-cell-mediated immunity, suppresses angiogenesis via Plexin-D1. *EMBO J.* 2007; 26:1373–1384. [PubMed: 17318185]
- Uesugi K, Oinuma I, Katoh H, Negishi M. Different requirement for Rnd GTPases of R-Ras GAP activity of Plexin-C1 and Plexin-D1. *J Biol Chem.* 2009; 284:6743–6751. [PubMed: 19136556]

- Wilkinson RN, Pouget C, Gering M, Russell AJ, Davies SG, Kimelman D, Patient R. Hedgehog and Bmp polarize hematopoietic stem cell emergence in the zebrafish dorsal aorta. *Dev Cell*. 2009; 16:909–916. [PubMed: 19531361]
- Williams CK, Li JL, Murga M, Harris AL, Tosato G. Up-regulation of the Notch ligand Delta-like 4 inhibits VEGF-induced endothelial cell function. *Blood*. 2006; 107:931–939. [PubMed: 16219802]
- Yee CS, Chandrasekhar A, Halloran MC, Shoji W, Warren JT, Kuwada JY. Molecular cloning, expression, and activity of zebrafish semaphorin Z1a. *Brain Res Bull*. 1999; 48:581–593. [PubMed: 10386838]

Highlights

Sema-PlxnD1 signaling promotes expression of the secreted VEGF decoy *sflt1*

Sema-PlxnD1 signaling allocates angiogenic capacity in the trunk's arterial tree

Sema-PlxnD1 signaling limits angiogenic responses within sprouts

Sema-PlxnD1 and Notch signaling play distinct roles in SeA angiogenesis

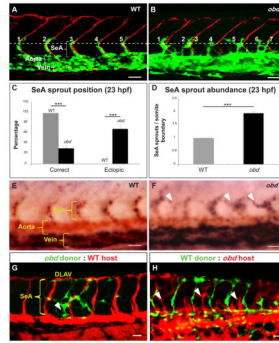


Figure 1. Sema-PlxnD1 signaling is cell autonomously required within the endothelium for proper SeA sprout abundance and distribution

(A–B) 23 hpf vasculatures, green. SBs, red. Horizontal myoseptum (HM), white dotted line. SeA sprouts, numbered. (A) WT. (B) *obd*. SeA sprout position (C) and abundance (D) in 23 hpf WT and *obd*. (E–F) WISH, 28 hpf trunks. Ectopic SeA sprouts, white arrowheads. Riboprobes: *flt4* (blue), *cdh5* (red). WT (E). *obd* (F). (G–H) 32 hpf chimeric vasculatures with ECs of donor (green) and host (red) origin. Examples of ectopic SeA sprouts, white arrowheads. (C–D) $n = 8$ WT, 12 *obd*. Error bars, s.e.m. *** $p < 0.001$. (E–F) $n = 10/10$ WT, 10/10 *obd*. (A–B, E–H) Anterior, left; dorsal, up. Scale bars, 30 μm . See Figure S1.

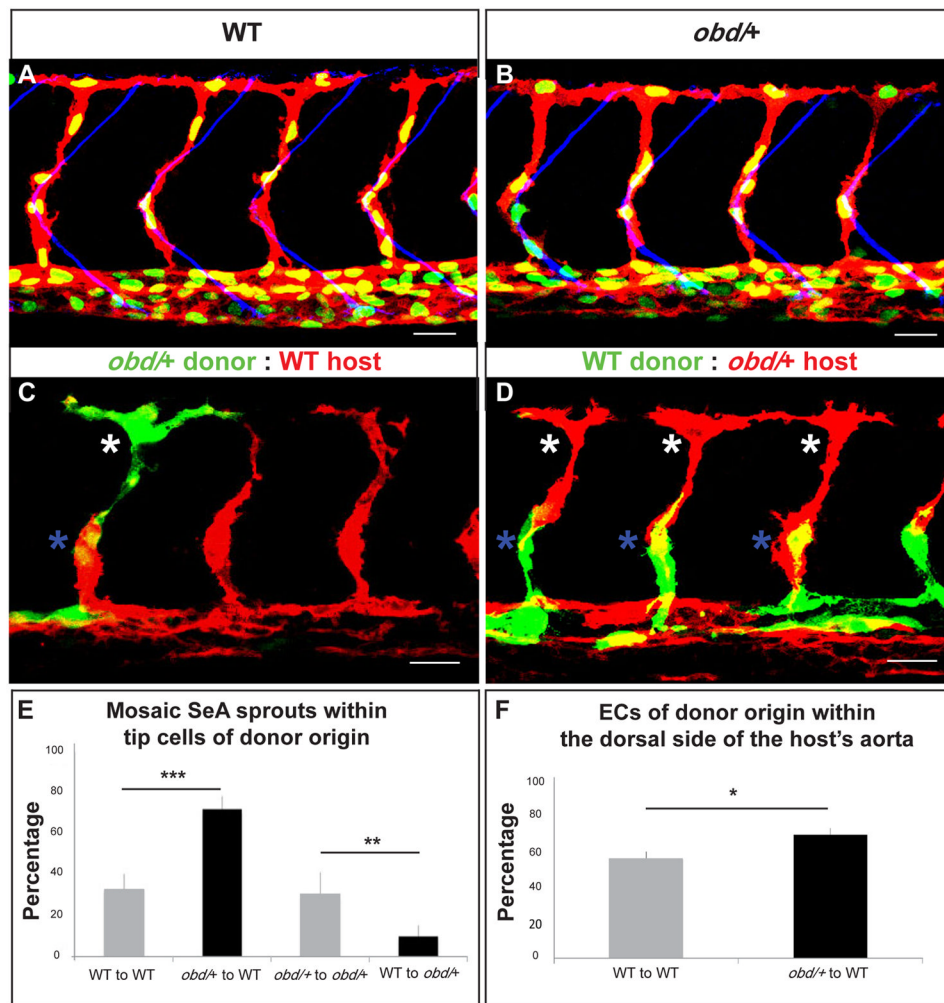


Figure 2. ECs with less Sema-PlxnD1 signaling tend to become tip cells and occupy the aorta's dorsal side
 (A–B) 32 hpf vasculatures. EC nuclei (green), membranes (red). SBs, blue. (A) WT. (B) *abd/+*. (C–D) 28 hpf vasculatures with ECs of donor (green) and host (red) origin. Asterisks: Tip cells (white), stalk cells (blue). (E) Percentage of mosaic SeAs with tip cells of donor origin in homogenotypic (grey bars) and heterogenotypic (black bars) chimeras. (F) Percentage of ECs of donor origin found within the dorsal side of the host's arterial tree in homogenotypic (grey bar) and heterogenotypic (black bar) chimeras. (E–F) * $p < 0.05$, ** $p < 0.01$, *** $p < 0.001$. Error bars, s.e.m. (E) $n = 27$ WT to *abd/+*, $n = 18$ *abd/+* to *abd/+*, $n = 38$ *abd/+* to WT, $n = 34$ WT to WT. Error bars, s.e.m. (F) $n = 24$ WT to WT, $n = 32$ *abd/+* to WT. (A–D) Anterior, left; dorsal, up. Scale bars, 30 μ m. See Figure S2 and Movie S1.

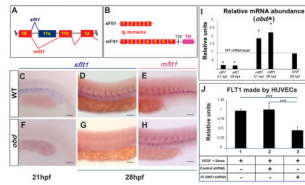


Figure 3. Sema-PlxnD1 signaling ensures the proper endothelial abundance of *sflt1*
(A) Alternative *flt1* splicing yields *sflt1* and *mflt1* isoforms with unique eleventh exons. Exons, colored boxes. Introns, black lines. **(B)** *sflt1* encodes a soluble 474 aa protein. *mflt1* encodes a 1,273 aa transmembrane protein. Protein domains: Immunoglobulin (Ig, red numbered boxes), transmembrane (TM, grey box), tyrosine kinase (TK, pink box). **(C–H)** WISH, embryo trunks (genotypes and ages indicated) hybridized with *sflt1* (**C–D**, **F–G**) and *mflt1* (**E**, **H**) riboprobes (blue). **(I)** qPCR measurements. Relative mRNA abundance of *sflt1*, *mflt1* and YFP (from *Tg(flt1:YFP)^{hu4624/+}*) in 28 hpf *obd/+* (WT level = 1, dashed line). Error bars, coefficient of variance * $p < 0.05$. **(J)** ELISA-based quantification of FLT1 prepared from cell extracts of HUVECs treated with both VEGF and Sema3E and the control or *PLXND1*-targeting shRNAs. Error bars, s.e.m. *** $p < 0.001$. **(C–H)** $n = 10$ embryos per riboprobe, stage and genotype. Pictures of representative examples of stainings observed (10/10 embryos in each category). Anterior, left; dorsal, up. Scale bars, 50 μ m. See Figure S3.

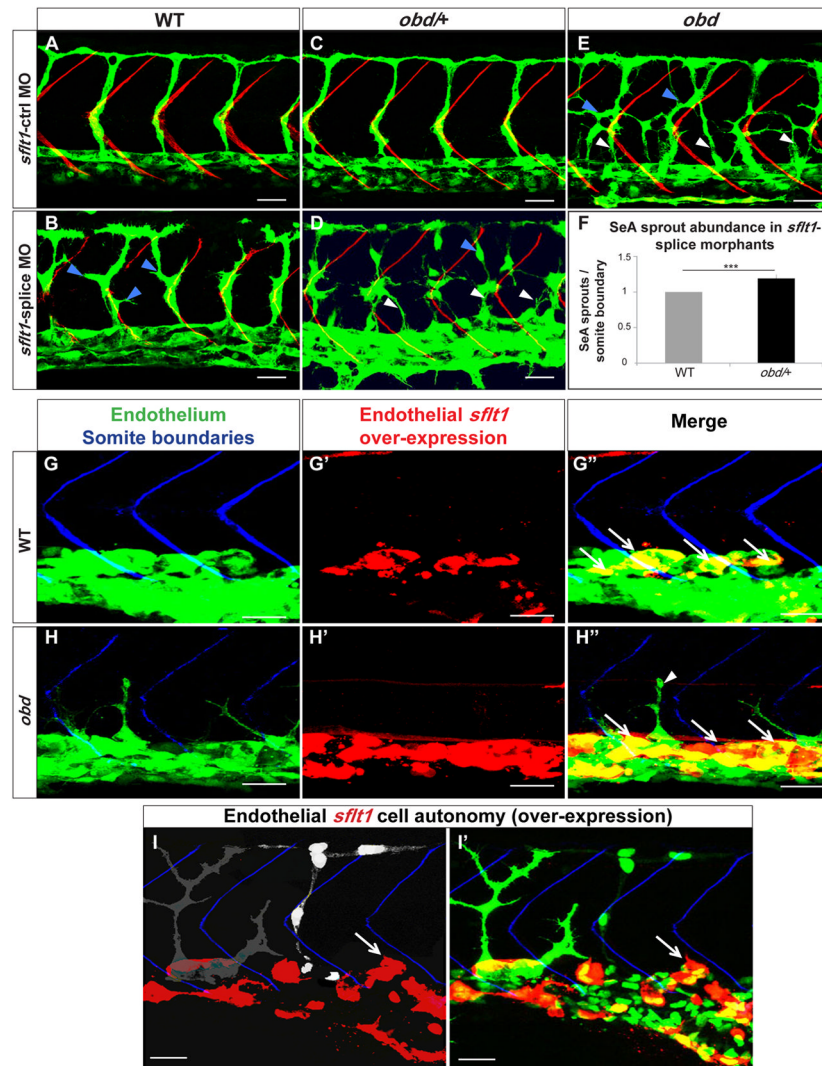


Figure 4. *plxnD1* and *sflt1* interact genetically, *sflt1* limits SeA angiogenesis cell autonomously (A–I) 32 hpf trunk vasculatures, green. (A–E) SBs, red. White arrowheads, ectopic SeA sprouts. Blue arrowheads, ectopic SeA branching. (A, C, E) Embryos treated with 20 ng of *sflt1*-ctrl MO: WT (A), *obd*/*+* (C), *obd* (E). Embryos treated with 20 ng of *sflt1*-splice MO: WT (B), *obd*/*+* (D). (F) 23 hpf SeA sprout abundance in WT (left, grey bar) and *obd*/*+* (right, black bar) *sflt1*-splice morphants. $n = 20$ WT and $n = 19$ *obd*/*+*. Error bars, s.e.m. $***p < 0.001$. (G–I') SBs, blue. GAL4FF/*UAS*-mediated endothelial-specific *sflt1* over-expression, red. White arrows, missing SeA sprouts. (G'–H'') Endothelial *sflt1* over-expression inhibits SeA sprouting. WT (G–G''). *obd* (H–H''), note lack of *sflt1* over-expression (red) in remaining SeA sprout (white arrowhead). (I–I') Mosaic vasculature with ECs from both *obd* donor and WT host. Endothelial-specific and mosaic *sflt1* and DsRed co-expression restricted to the WT endothelium (red, I–I'). *obd* ECs express cytosolically-targeted EGFP (grey in I; green in I'). WT ECs express nuclear-targeted EGFP (white in I; green in I'). *obd* and WT ECs without *sflt1* over-expression (DsRed⁻) from SeA sprouts even next to *sflt1* over-expressing WT ECs (DsRed⁺). WT ECs over-expressing *sflt1* (DsRed⁺) fail to form SeA sprouts (white arrows, I–I'). (G–H'') $n = 30$ embryos with over-expression per genotype, all showing suppression of SeA sprouting. Anterior, left; dorsal, up. Scale bars, 30 μ m. See Figure S4.

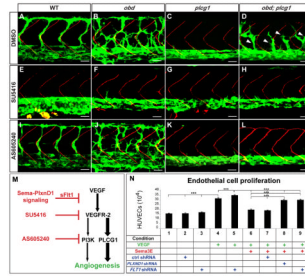


Figure 5. Enhanced VEGF signaling causes *obd*'s exacerbated SeA angiogenesis
A–L, 32 hpf trunk vasculatures. WT, *obd*, *plc1* and *obd; plc1* treated with DMSO, SU5416 (VEGFR inhibitor) or AS605240 (PI3K inhibitor). Genotypes, top; treatments, left. Endothelium, green. SBs, red. White arrowheads, recovered SeA sprouts in *obd; plc1*. Anterior, left; dorsal, up. Scale bars, 30 μ m. n = 18 embryos per genotype and treatment. Pictures show representative phenotypes (18/18 embryos per category). **(M)** Diagram of the VEGF cascade and steps inhibited by *sft1* and drugs used in **(E–L)**. **(N)** HUVEC proliferation in response to combinations of VEGF, Sema3E and shRNAs (control, *PLXND1* and *FLT1*). *** $p < 0.001$. Error bars, s.e.m. See Figure S5.

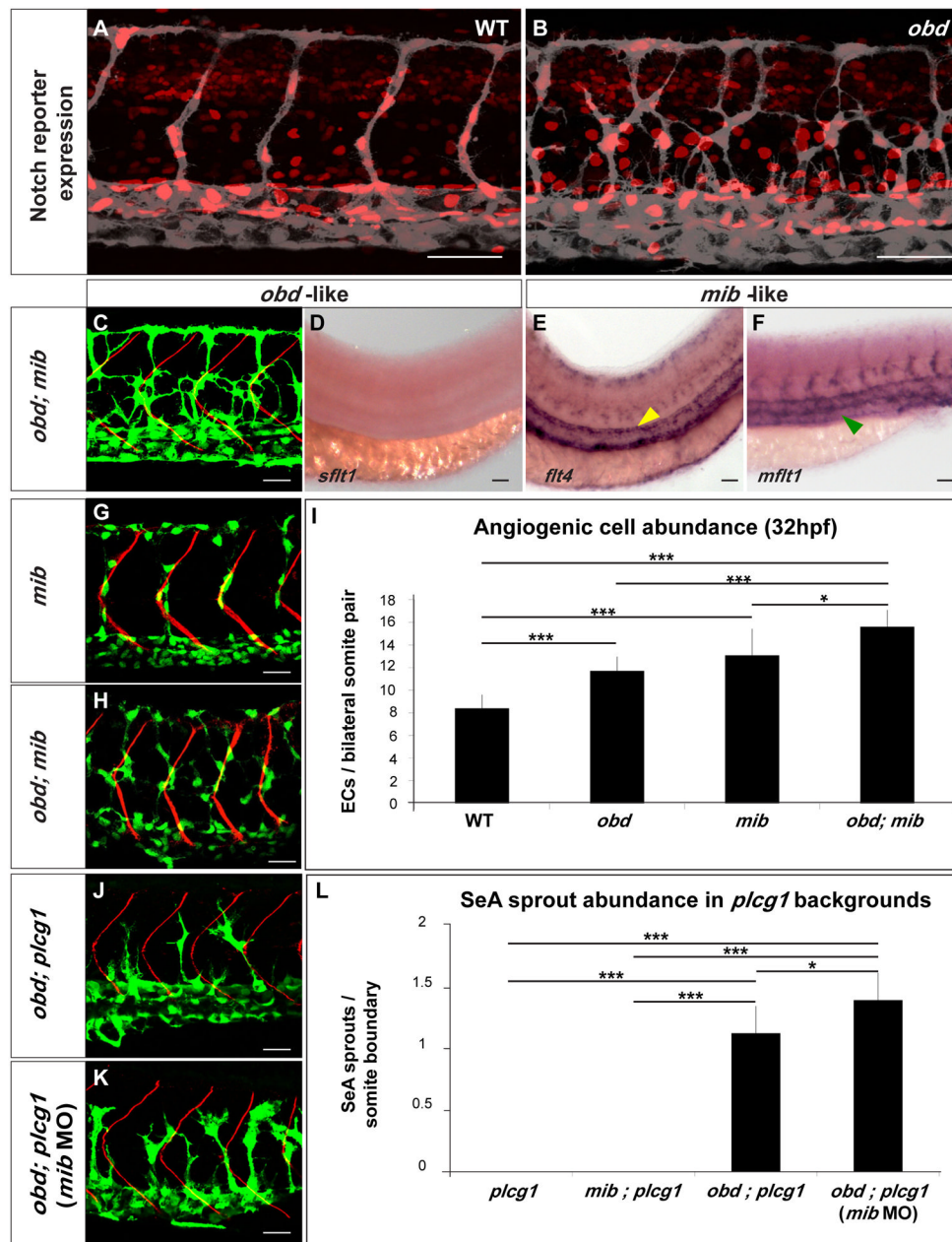


Figure 6. Notch signaling loss does not phenocopy *obd*
 (A–B) Expression of Notch’s activity nuclear reporter *Tg(Tp1bglob:hmgb1-mCherry)^{jh11}* (red) in the endothelium (grey) of WT (A) and *obd* (B). (C–F) *obd; mib*. (C) Endothelium, green. SBs, red. (D–F) WISH with *sflt1*, *flt4* and *mflt1* riboprobes, as indicated. Double mutant phenotypes classified as *obd*-like (C–D) or *mib*-like (E–F) based on the mutant they resemble most. Note lack of *sflt* (as in Fig. 3G) and ectopic aortic *flt4* (yellow arrowhead; as in Fig. S6A) and venous *mflt1* stainings (green arrowhead, as in Fig. S6B). (G–I) Angiogenic cell abundance within the trunk’s arterial tree of WT, *obd*, *mib* (G) and *obd; mib* (H) in *Tg(fli1:nEGFP)^{y7}* embryos. (G–H) EC nuclei, green. SBs, red. (I) Quantification; n= 10 per genotype. (J–L) SeA sprout abundance in *plcg*, *mib; plcg*, *obd; plcg* (J) and *obd; plcg* embryos injected with 10 ng of *mib* MO (*mib* MO) (K). (J–K) Endothelium, green. SBs, red. (L) n = 8, 7, 11 and 9 for *plcg*, *mib; plcg*, *obd; plcg* and *obd; plcg (mib MO)*,

respectively. Scale bars: 50 μm (**A–B**, **D–F**), 30 μm (**C**, **G–H**, **J–K**). (**I**, **L**) $*p < 0.05$, $***p < 0.001$. Error bars: s.e.m. (**A–F**, **G–H**, **J–K**) Anterior, left; dorsal, up. Trunk images and quantifications: 32 hpf (**A–C**, **G–L**), 28 hpf (**D–F**). See Figure S6.

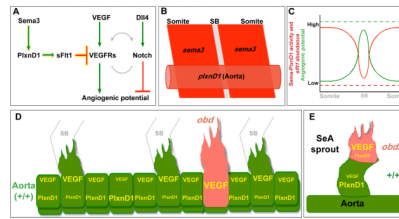


Figure 7. Model for how Sema3-PlxnD1 signaling restricts angiogenic potential along the aorta and limits angiogenic responses within SeA sprouts

(A) Sema3-PlxnD1 signaling inhibits VEGF's pro-angiogenic effects via sFlt1, limiting angiogenic potential. The complex cross-regulation (grey lines) between the VEGF and Notch cascades implies Sema-PlxnD1 signaling impacts Notch activity indirectly. (B) Somitic *sema3s* (dark red) and endothelial *plxnD1* (light red) expression precedes SeA sprouting (SB, grey) (Roos et al., 1999; Torres-Vazquez et al., 2004; Yee et al., 1999). (C) WT aortic Sema-PlxnD1 signaling levels (red solid line) are highest in ECs next to the somites and lowest in ECs next to SBs, where angiogenic potential (green solid line) is highest. *obd* lacks Sema-PlxnD1 activity and thus *sflt1* abundance is greatly reduced (red dotted line), leading to uniformly enhanced angiogenic potential levels (green dotted line) that yield too many and ectopic SeA sprouts. (D–E) VEGF signaling and angiogenic responses are cell autonomously enhanced by loss (*obd*) or decreased (*obd/+*) endothelial *plxnD1* activity, as exemplified by *obd* to WT (D) and *obd/+* to WT (E) chimeras. VEGF signaling and PlxnD1 activity levels are indicated by font size.